β^- decay of neutron-rich ^{45}Cl located at the magic number $N = 28$

Soumik Bhattacharya,[1,*] Vandana Tripathi,[1,†] S. L. Tabor,[1] A. Volya,[1] P. C. Bender,[2] C. Benetti,[1] M. P. Carpenter,[3] J. J. Carroll,[4] A. Chester,[5,6] C. J. Chiara,[4] K. Childers,[5,7] B. R. Clark,[8] B. P. Crider,[8] J. T. Harke,[9] R. Jain,[6,10] S. N. Liddick,[5,6,7] R. S. Lubna,[6] S. Luitel,[8] B. Longfellow,[5,10] M. J. Mogannam,[5] T. H. Ogunbeku,[5,6,8] J. Perello,[1] A. L. Richard,[5,9] E. Rubino,[1] S. Saha,[2] O. A. Shehu,[8] R. Unz,[8] Y. Xiao,[5,8] and Yiyi Zhu[2]

[1]*Department of Physics, Florida State University, Tallahassee, Florida 32306, USA*
[2]*Department of Physics, University of Massachusetts Lowell, Lowell, Massachusetts 01854, USA*
[3]*Physics Division, Argonne National Laboratory, Argonne, Illinois 60439, USA*
[4]*U.S. Army Combat Capabilities Development Command Army Research Laboratory, Adelphi, Maryland 20783, USA*
[5]*National Superconducting Cyclotron Laboratory, Michigan State University, East Lansing, Michigan 48824, USA*
[6]*Facility for Rare Isotope Beams, Michigan State University, East Lansing, Michigan 48824, USA*
[7]*Department of Chemistry, Michigan State University, East Lansing, Michigan 48824, USA*
[8]*Department of Physics and Astronomy, Mississippi State University, Mississippi State, Mississippi 39762, USA*
[9]*Lawrence Livermore National Laboratory, Livermore, California 94550, USA*
[10]*Department of Physics and Astronomy, Michigan State University, East Lansing, Michigan 48824, USA*

(Received 28 April 2023; revised 5 July 2023; accepted 26 July 2023; published 18 August 2023)

Results from the study of the β^- decay of ^{45}Cl, produced in the fragmentation of a 140-MeV/u ^{48}Ca beam, are presented. The half-life for ^{45}Cl β decay is measured to be 513(36) ms. The β^- and β^-1n decay of ^{45}Cl populated excited states in ^{45,44}Ar, respectively. On the basis of γ-ray singles and γ-γ coincidence data, decay schemes for the two daughter nuclei have been established. They are compared with shell model calculations using the FSU interaction. The low-lying negative parity states for ^{45}Ar are well described by a single particle (neutron) occupying orbitals near the Fermi surface, whereas neutron excitations across the $N = 20$ shell gap are needed to explain the positive-parity states which are expected to be populated in allowed Gamow-Teller β decay of ^{45}Cl. The highest β feeding to the $5/2^+$ state in ^{45}Ar from the ground state of ^{45}Cl points towards a $3/2^+$ spin-parity assignment of the ground state of the parent over the other possibility of $1/2^+$. The high Q_{β^-} value of ^{45}Cl decay allows for the population of $1p1h$ states above the neutron separation energy in ^{45}Ar leading to positive parity states of ^{44}Ar being populated by removal of one neutron from the *sd* shell. The spin-parities of the excited levels in ^{44}Ar are tentatively assigned for the first time by comparison with the shell model calculations. The 2978 keV level of ^{44}Ar is identified as the excited 0^+ level which could correspond to a different configuration from the ground state.

DOI: 10.1103/PhysRevC.108.024312

I. INTRODUCTION

In the past few decades a primary focus of nuclear structure studies has been understanding whether the known magic numbers that appear to hold good near stability remain so as the drip lines are approached [1–3] where the proton-neutron asymmetry is large. The magic numbers $N = 28$ and $Z = 28$ are the lowest ones whose emergence requires a strong spin-orbit interaction and thus are of particular interest for the experimental and theoretical study of exotic nuclei far from stability to understand the isospin dependence of the spin-orbit interaction. There are several examples of experimental evidence, accompanied by theoretical calculations, which indicate that the $N = 28$ shell gap below ^{48}Ca reduces continuously with decreasing proton number. Just two protons away from ^{48}Ca, the excitation energy of the first 2^+ state in ^{46}Ar drops considerably [4]. Further, around doubly magic ^{48}Ca, which is considered spherical, the nuclear shape changes rather rapidly to develop deformation in ^{42}Si [5] while shape coexistence is observed in ^{44}S [6–11].

The study of the excitation of protons in odd-Z nuclei through measurements of excited states in the K, Cl, and P isotopes has indicated a near-degeneracy of the proton $d_{3/2}$ and $s_{1/2}$ orbitals approaching $N = 28$ [12]. The increase of collectivity away from $Z = 20$ as well as the degeneracy of $\pi d_{3/2}$ and $\pi s_{1/2}$ orbitals can be explained by the monopole part of the tensor force [13], which is attractive between the $\nu f_{7/2}$ and $\pi d_{3/2}$. With the degeneracy of the two proton orbitals, the ground states of odd-A Cl isotopes are found to vary between $3/2^+$ and $1/2^+$. The ground state spin-parity of ^{45}Cl is not known experimentally, though both $1/2^+$ [12] and $3/2^+$ [14] are predicted as possible spins based on different calculations. The ground states of odd-A $^{37-45}$Ar, ($Z = 18$) isotopes on the other hand are anticipated to be $7/2^-$ in a simple filling of the orbitals due to a neutron hole in the

*Corresponding author: soumik.kgpiit@gmail.com
†Corresponding author: vtripath@fsu.edu

$f_{7/2}$ orbital. However, the ground state spin/parity changes between $5/2^-$ and $7/2^-$ throughout the Ar isotopic chain from $N = 20$ to $N = 28$. A charge radius measurement using laser spectroscopy has found the ground state as $7/2^-$ for ^{39,41}Ar, $5/2^-$ for ^{43}Ar [15], and then again $7/2^-$ for ^{45}Ar [16].

The $N = 26$ ^{44}Ar is proposed to be deformed with a prolate ground state associated with a high $B(E2)$ value for the 2_1^+ to 0_1^+ transition from Coulomb excitation study [17,18]. The $B(E2)$ value for the same transition in ^{46}Ar [4,19] on the other hand is found to be lower supporting the smaller charge radius for the ^{46}Ar [15] compared to ^{44}Ar. However, the latest measurement of the $B(E2)$ values from the lifetime measurement of the 2_1^+ state for ^{46}Ar and ^{44}Ar by Mengoni *et al.* [20], reports almost double $B(E2)$ values for the ^{46}Ar than ^{44}Ar which is unexpected if the $N = 28$ shell gap persists for ^{46}Ar. Different calculations also show a discrepancy between the $B(E2)$ values of these two nuclei which remains to be resolved. Between the deformed ^{44}Ar and near spherical ^{46}Ar, the structure of the intermediate ^{45}Ar is therefore of special interest.

β-decay is an excellent experimental tool to study the excited states of neutron rich nuclei near $N = 28$. The large Q_{β^-} values ensure that a large number of excited states, both bound and unbound, are populated. In this region of the chart of nuclides, the differences in ground-state spins and parities between the β-decay parent and daughter limit the possibility of direct feeding to the ground state. This is due to the protons filling the $1s_{1/2}$ or $0d_{3/2}$ subshells, whereas the neutrons are filling the $0f_{7/2}$ subshell. For odd-A Cl isotopes like ^{45}Cl in this work, a positive-parity ground state is expected, which will decay to the positive-parity excited states of odd-A daughter Ar via allowed Gamow-Teller (GT) transitions and not feed the negative parity ground state directly. The positive-parity states in the even-odd daughter arise from promoting a proton or a neutron across the $Z = 20$ or $N = 20$ shell gap and these $1p1h$ states are expected at relatively high energies. For ^{45}Cl, the expected $3/2^+$ ground state will β-decay to positive-parity ($1/2^+$, $3/2^+$, or $5/2^+$) or negative-parity ($1/2^-$, $3/2^-$, or $5/2^-$) states by allowed or first forbidden β decays, respectively. Figure 1 illustrates the possible decay scheme of ^{45}Cl. With the large Q_{β^-} value, the β decay can also populate states above the neutron separation energy (S_n) in ^{45}Ar and therefore opens up the possibility of studying the excited states in the $\beta 1n$ daughter ^{44}Ar. The investigation of excited states in ^{44,45}Ar is the focus of this study along with the ground state spin and parity determination for the parent ^{45}Cl.

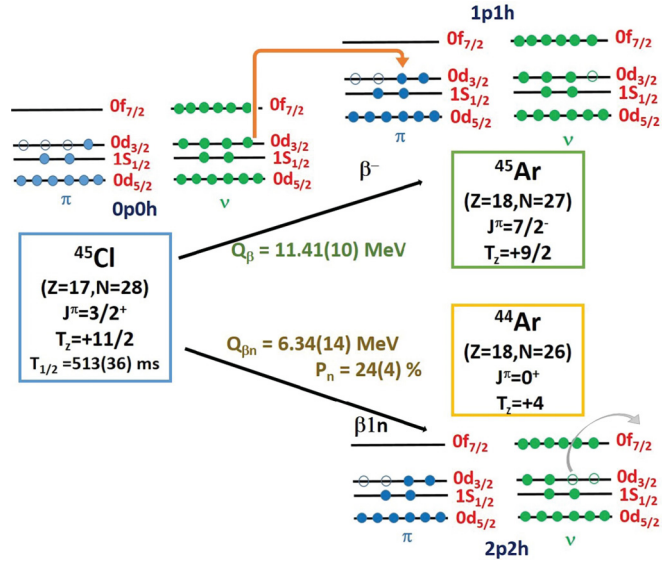

FIG. 1. Schematic representation of ^{45}Cl decay via $\beta 0n$ and $\beta 1n$ channels. The boxes display the ground-state spin-parity assignments of the corresponding nuclei. The dominant neutron and proton configuration for the ground state of parent nucleus ^{45}Cl and the excited states expected to be populated in ^{45}Ar and ^{44}Ar by β and $\beta 1n$ are shown. The arrows show the transformation of neutron from ^{45}Cl to proton and removal of neutron from ^{45}Ar involving the possible orbitals to produce excited states of ^{45}Ar and ^{44}Ar, respectively.

II. EXPERIMENTAL SETUP

The experiment was carried out at the National Superconducting Cyclotron Laboratory (NSCL) [21] at Michigan State University to investigate the β^- decay of exotic ^{45}Cl. A 140-MeV/u ^{48}Ca primary beam, was fragmented using a thick Be target at the target position of the fragment separator, A1900 [22], to produce the nuclei of interest. A wedge-shaped Al degrader, which increases the energy dispersion for different fragments, was placed at the intermediate dispersive image of the A1900 separator to provide a cleaner particle identification of the cocktail beam.

After passing through the wedge shaped Al degrader, the selected isotopes were transported to the Beta Counting System (BCS) [23]. The BCS is equipped with a 986 μm thick pixelated (40 strips ×40 strips) double-sided silicon strip detector (DSSD) at the center. An Al degrader upstream reduced the energy of the fragments to ensure that the implants stopped at the middle of the DSSD. The DSSD was followed by a single-sided silicon strip detector (SSSD) which served as a veto detector. This veto detector was used to counter a large flux of light particles which were transmitted through the DSSD detector for the particular A1900 settings used for this experiment which can impair implant-β correlations. Dual-gain preamplifiers were used for the DSSD to record the time and position of implants (GeV energy depositions), as well as subsequent decays (keV to MeV energy depositions). The implant rate was kept well below 200/sec to maximize the efficiency of correlating the implanted ion with the decay products.

Two Si PIN detectors, placed upstream of the DSSD, provided the partial energy loss information of the fragments. Along with the scintillator at the intermediate dispersive image of the A1900 these PIN detectors provide the time of flight information used to generate particle identification plots (PID) of the incoming implants as shown in Fig. 2. The DSSD and SSSD detector combination was surrounded by 16 Clover detectors to detect the β-delayed γ rays with an efficiency of about 5% at 1 MeV. The efficiency of the array was measured with the SRM [24] (standard reference material—

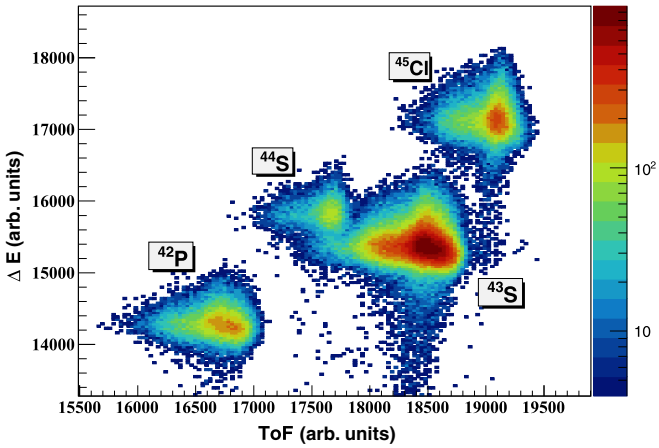

FIG. 2. The two-dimensional plot of partial energy deposition in the upstream Si PIN detector (ΔE) and the time of flight (ToF) measurement with respect to the focal plane scintillator detector used for particle identification of the nuclei of interest in the present work.

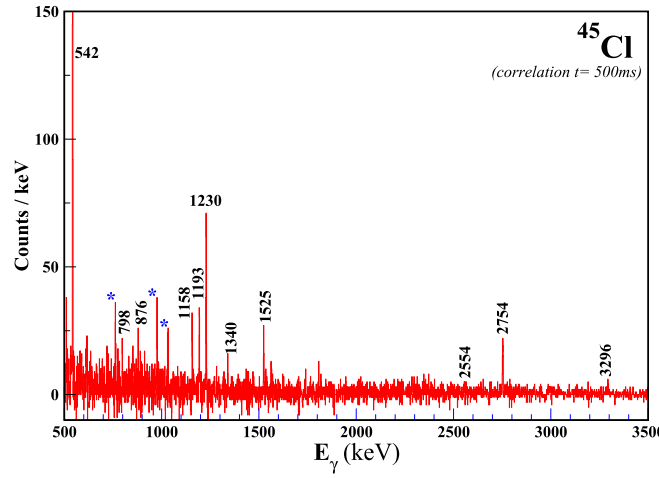

FIG. 3. A typical fragment-β-γ correlated spectrum which clearly shows the strong γ transitions belonging to ^{45}Ar and ^{44}Ar. The spectrum was generated for a correlation window of 500 ms between the ^{45}Cl blob as seen in the PID and corresponding β particles after subtracting background from a long correlation window. The asterisks mark background transitions pertaining to the strongest fragment of the cocktail beam.

consisting of radioactive ^{125}Sb, ^{125}Te, ^{154}Eu, ^{155}Eu) and ^{56}Co sources placed outside of the DSSD and then corrected for the dimensions of the DSSD with GEANT4 simulations. The time-stamped data were collected using the NSCL digital data acquisition system [25]. The timing and spatial correlations from each channel corresponding to the different detectors were used to ensure the correlation between the implanted fragments in the DSSD and the corresponding β-decay event.

III. EXPERIMENTAL RESULTS

Figure 2 shows the clear separation of the different isotopes produced in the present experimental investigation. Selected ^{45}Cl implants from the cocktail beam were correlated with the emitted β particles to obtain half-life. Further, coincidence of delayed γ transitions with the correlated implant-decay events allowed us to study the excited states of ^{45}Ar and ^{44}Ar produced via β and β-1n decay respectively. A typical fragment-β-γ correlation spectrum for ^{45}Cl decay can be seen in Fig. 3, where the correlation window between implant and β particle is 500 ms and the γs are in prompt coincidence with the decay particles. Intense transitions depopulating the excited states of ^{45}Ar and ^{44}Ar are marked. Contamination from the strongest populated channel (^{43}S decay) via random correlations are also observed in this case and those transitions are marked with an asterisk. The β decay of other neutron rich P and S nuclei seen in Fig. 2 have been reported and discussed in our previous publication [26].

A. β decay of ^{45}Cl

The time differences between ^{45}Cl implants and β particles detected in the same or one of the adjacent eight pixels of the DSSD, in coincidence with the strongest ground-state γ transition (542 keV) in ^{45}Ar, were histogrammed to generate a decay curve. The half-life of ^{45}Cl was extracted from this decay curve, as shown in Fig. 4. A fit using a exponential decay function of ^{45}Cl and a background component accounting for other long-lived activity gives a half-life of 513(36) ms. The previous half-life measurement for ^{45}Cl with a value of 400(43) ms is taken from the work of Sorlin *et al.* [27] whereas a preliminary work by Winger *et al.* [28] reported it as 420(30) ms. In Sorlin *et al.* the half-lives were deduced from constructing a time histogram of the β-n coincidences detected after the identification of the corresponding parent nucleus. For ^{45}Cl only 880 events were detected and the authors discuss a possible mixing with another implant with shorter half-life. The measured half-life of 513 (36) ms obtained in this work is consistent with the shell model calculations using the FSU

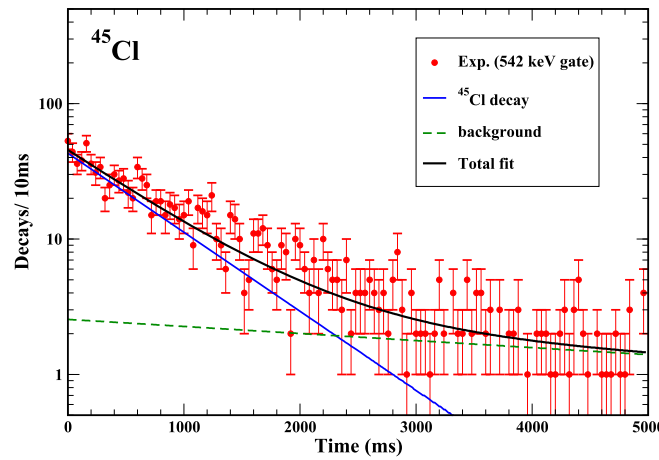

FIG. 4. The time difference between the ^{45}Cl implants and correlated β decay events gated by the 542-keV ground state transition in ^{45}Ar. The experimental data are fitted with exponential decay functions to account for ^{45}Cl decay with suitable background. The half-life is found to be $T_{1/2} = 513(36)$ ms. This number is larger than the previous measurements of 400(43) ms [27] and a preliminary number of 420(30) ms from Ref. [28] though within 2σ.

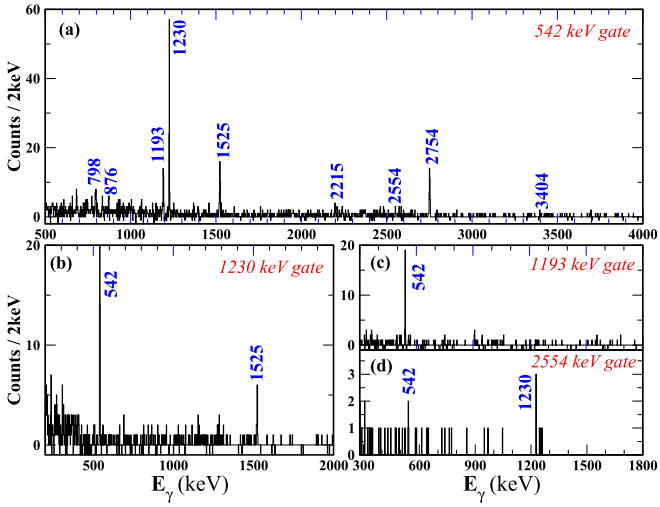

FIG. 5. (a)–(d) Coincidences observed between the γ transitions in ^{45}Ar used to establish the level scheme. A correlation window between the implant and decay equal to about five half-lives of the parent nucleus was used to record the γ transitions.

interaction which give a value of 500 ms without including the first forbidden β transitions.

The γ-γ coincidences between the transitions observed in ^{45}Ar are shown in Figs. 5(a)–5(d) and the corresponding level scheme in Fig. 6. Figure 5(a) displays the 542-keV gate which is the strongest transition in ^{45}Ar and one can see all the known transitions: 798, 876, 1193, 1230, 1525, and 2754 keV along with the newly placed 2554 keV. The 2554-keV

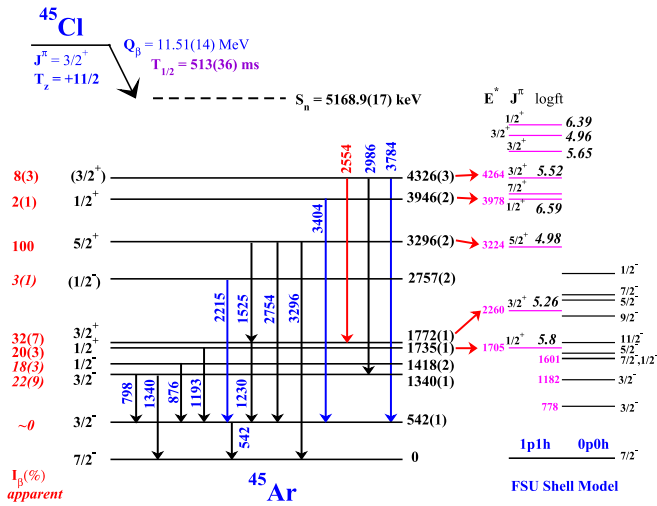

FIG. 6. Partial level scheme of ^{45}Ar following β^- decay of ^{45}Cl with a $T_{1/2} = 513(36)$ ms and $Q_{\beta^-} = 11.51(14)$ MeV. The transitions marked in black were known before whereas red indicates the new transition observed in this work. The blue marked transitions were reported earlier as tentative by Ref. [29] which we are able to verify and confirm. The apparent beta branching (relative to the $5/2^+$ state at 3296 keV) is also shown for the excited states. The shell model calculation using the FSU interaction [30] predicted the $0p0h$ and $1p1h$ excited states and are shown along with the experimental levels. See text for more details.

TABLE I. γ-ray energies along with the corresponding initial levels and initial and final spins for ^{45}Ar and ^{44}Ar observed in the present work are presented. For ^{45}Ar the intensities of the γ rays are normalized with respect to the strongest 542-keV γ ray. For ^{44}Ar the branching from each level is shown with each branch normalized to the strongest one from that level.

^{45}Ar E_i (keV)	$J_i \rightarrow J_f$	E_γ (keV)	I_{rel}
542(1)	$3/2^- \rightarrow 7/2^-$	542(1)	100(10)
1340(1)	$3/2^- \rightarrow 7/2^-$	1340(1)	10.6(12)
	$3/2^- \rightarrow 3/2^-$	798(2)	3.4(5)
1418(2)	$1/2^- \rightarrow 3/2^-$	878(1)	10.5(12)
1735(1)	$1/2^+ \rightarrow 3/2^-$	1193(1)	12.1(14)
1772(1)	$3/2^+ \rightarrow 3/2^-$	1230(1)	37.6(39)
2757(2)	$(1/2^-) \rightarrow 3/2^-$	2215(2)	1.8(4)
3296(2)	$5/2^+ \rightarrow 3/2^+$	1525(1)	16.5(18)
	$5/2^+ \rightarrow 3/2^-$	2754(1)	30.4(34)
	$5/2^+ \rightarrow 7/2^-$	3296(2)	12.6(16)
3946(2)	$1/2^+ \rightarrow 3/2^-$	3404(2)	0.9(3)
4326(3)	$(3/2^+) \rightarrow 3/2^+$	2554(2)	2.0(4)
	$(3/2^+) \rightarrow 3/2^-$	2986(2)	0.8(3)
	$(3/2^+) \rightarrow 3/2^-$	3784(3)	2.0(5)
^{44}Ar			Rel. branching
1158(1)	$2^+ \rightarrow 0^+$	1158 (1)	100
2011(1)	$(2^+) \rightarrow 2^+$	853(1)	68(24)
	$(2^+) \rightarrow 0^+$	2011(1)	100
2978(1)	$(0^+) \rightarrow (2^+)$	966(1)	100
	$(0^+) \rightarrow 2^+$	1818(1)	83(33)
4808(2)	$(2^+) \rightarrow (2^+)$	2797(2)	100
	$(2^+) \rightarrow 2^+$	3649(2)	4.3(12)
	$(2^+) \rightarrow 0^+$	4808(2)	4.7(16)
5354(2)	$(1^+) \rightarrow (0^+)$	2376(1)	100

transition is proposed to decay from the highest observed level, at 4326 keV to the 1772-keV level based on the coincidences shown in Fig. 5(d). The coincidence gate of 1230 keV shows the 542-keV and 1525-keV transitions only, which belong to the same cascade [Fig. 5(b)]. The absence of any transition other than 542 keV in the coincidence gate of 1193 keV confirms that no gamma transition is feeding the 1735-keV level [Fig. 5(c)]. In Ref. [29] two tentative γ transitions at 3408 and 2215 keV were reported to decay from the proposed 3950- and 2757-keV levels, respectively. The existence of the 3950-keV (3946 keV in present study) level was established prior from the neutron transfer study [16]. The present work confirms the presence of 2215- and 3404-keV transitions in the coincidence gate of 542 keV [Fig. 5(a)].

The level scheme in Fig. 6 shows the apparent relative β branching of the levels considering the absolute efficiencies of the detected γ rays. The assignment of the spin-parities of the observed levels of ^{45}Ar is guided by predictions from shell-model calculations (discussed later in detail) as well as from the γ branching and the allowed β transition rates from the parent nucleus (^{45}Cl). The β decay should primarily populate the $1p1h$ positive parity states and hence the logft values from the shell-model (SM) calculations are noted only for the positive parity states. Table I gives the level energies and

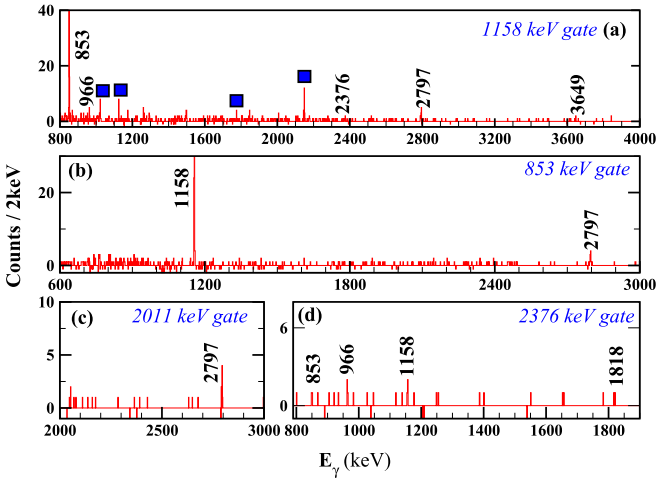

FIG. 7. (a)–(d) Coincidences observed between the γ transitions in ^{44}Ar. The 1158 keV transition coincidence gate shows contamination from ^{44}Ca which are marked with blue solid boxes.

γ rays decaying from them, possible J^π values, and relative intensities for both ^{45}Ar and ^{44}Ar excited states.

B. $\beta 1n$ decay of ^{45}Cl

The large $Q_{\beta^-} = 11.51$ MeV of ^{45}Cl, along with a low (5.169-MeV) neutron separation energy (S_n) of ^{45}Ar, leads to a significant beta-delayed neutron branch populating excited states in ^{44}Ar. The spin-parities of the states populated in the β-delayed daughter largely depend on the spin-parity of excited state in ^{45}Ar.

The γ rays in coincidence with the 1158-keV ground-state transition (2^+ to 0^+) in ^{44}Ar are shown in Fig. 7(a). Here, it is worth mentioning that a close by γ transition (1157 keV) exists in ^{44}Ca (2^+ to 0^+ transition) leading to some spurious coincidences marked with solid blue boxes in Fig. 7(a). The strongest transition seen is 853 keV, which is the decay from the second 2^+, 2011 keV level to the first excited 2^+ (1158-keV) level. This second 2^+ state at 2011 keV has been confirmed in an earlier deep inelastic reaction study by Wan *et al.* [31]. The coincidence spectrum also shows the weaker 966-, 2376-, 2797-, and 3649-keV transitions which were already reported in Ref. [29]. The presence and absence of the 3649-keV transition in the 1158 and 853 gates, respectively, fixes the placement of this transition from the 4808 keV to the 1158 keV level. The highest observed excited level 5354 keV from the present work is seen to be decaying only to 2978 keV level via the 2376 keV transition.

The level scheme, formed from the present work is shown in Fig. 8 (left panel). Along with the experimental levels, the corresponding SM predicted levels (right panel) are also shown. All the transitions, apart from the 853-, 1158-, and 2011-keV transitions are observed for the first time in the $\beta 1n$ decay of ^{45}Cl and are marked in blue in the experimental level scheme shown in Fig. 8 (left panel). Two levels at 2746 keV and 3439 keV, shown in the experimental level scheme by green dashed lines, were not populated in the βn channel but are shown for comparison with the shell model calculations and were seen in the previous study by Fornal *et al.* [32].

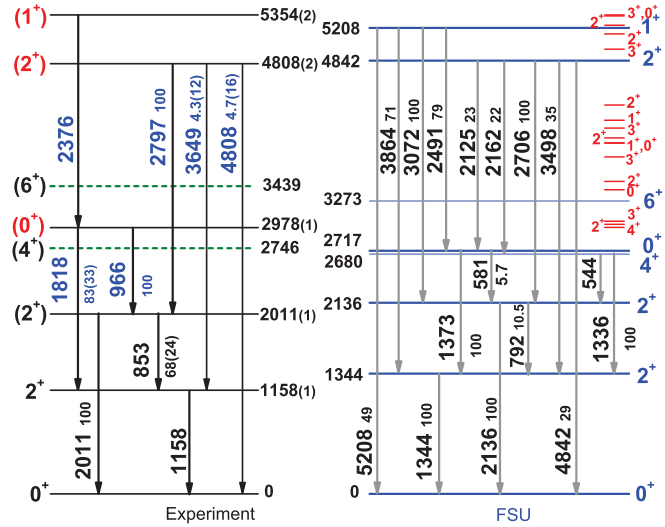

FIG. 8. Partial level scheme of ^{44}Ar following $\beta 1n$ decay of ^{45}Cl [$Q_{\beta^- n} = 6.34(14)$ MeV] is shown in the left panel. The relative intensity of the de-exciting transitions (except the 1158 keV) are also reported along with the associated errors. Two levels are shown by green dashed lines which were reported previously but not seen in the present work. The transitions which are seen for the first time from $\beta 1n$ work are marked in blue. The spins of the levels that are suggested for the first time in the present work are marked with red (see Sec. IV B). Predictions of shell-model (SM) calculations using the FSU interaction [30] are shown in the right panel. The possible γ transitions and their relative branching ratios were also calculated and are noted. The excited states, predicted by the SM but not observed in the experiment, are shown at the right of the SM level scheme in red.

IV. DISCUSSION

A. ^{45}Ar

The ground state spin-parity of ^{45}Cl is expected to be $3/2^+$ due to an odd proton in $d_{3/2}$ orbital and a full $\nu f_{7/2}$ orbital in a simple picture as illustrated in Fig. 1. However with the $d_{3/2}$ and $s_{1/2}$ orbitals being nearly degenerate, a $1/2^+$ assignment cannot be ruled out. Below, based on the γ decay characteristics and shell-model calculations, we suggest a $3/2^+$ spin-parity. The shell-model calculations presented in this work were performed using the shell model code CoSMo [33] using the FSU interaction. The FSU interaction (shell-model interaction developed at Florida State University) is an empirical effective interaction obtained by fitting experimental data in the $0p$-$1s0d$-$0f1p$ valence space, with details provided in Ref. [30]. It is aimed to explain cross-shell excitations between the *sd* and *fp* shell and also *p* and *sd* shells for neutron-rich *sd*-shell nuclei [30]. The predictions of the FSU interaction have found great success in explaining many experimental observations [34,35]. For the calculations quoted here, when the excitations are confined to the *sd* shell for both neutrons and protons they are referred to as $0p0h$ excitations, whereas $1p1h$ calculations involve excitation of single nucleon across either the $N = Z = 8$ ($0p$-$1s0d$) shell gap or the $N = Z = 20$ ($1s0d$-$0f1p$) gap creating opposite parity states.

TABLE II. SM predictions (using the FSU interaction) for the branching ratio of the $5/2_1^+$ state in ^{45}Ar. The experimental value of the γ ray transition was used in the calculation of the rates. The difference in branching to the $3/2^+$ and $1/2^+$ states is used to confirm the spin-parity assignment to the two experimental state at ≈1.7 MeV.

$J_i \rightarrow J_f$	E_γ (keV)	$B(M1)$ (μ_N^2) rate(1/sec)	$B(E2)(e^2\text{fm}^4)$ rate(1/sec)
$5/2^+ \rightarrow 1/2^+$	1525		104
			1.05×10^{12}
$5/2^+ \rightarrow 3/2^+$	1525	0.35	27.3
		2.19×10^{13}	2.77×10^{10}

1. Positive-parity states

From the selection rules of allowed GT decay, states with positive parity should have the highest branching in the daughter nucleus. In a more nuanced picture, the β^- decay will likely involve the conversion of a $d_{3/2,5/2}$ neutron into a $d_{3/2}$ proton as ^{45}Ar has a vacancy in the $\pi d_{3/2}$ orbital. The other possibility is for the $s_{1/2}$ neutron to transform into an $s_{1/2}$ proton as indicated in Fig. 1. These will create neutron hole states in ^{45}Ar corresponding to the $1p1h$ states in the shell-model calculations. We propose that the states at 1735-, 1772-, 3296-, 3946-, and 4326 keV with the highest branching to be populated via allowed GT transitions and hence have positive parity. In a recent transfer study using the reaction ^{1}H(^{46}Ar, d)^{45}Ar [16] the same states except 4326 keV were proposed as neutron hole states. However, in their excitation energy spectrum, there are indications of a weak 4.3 MeV state overlapping with the 3.95 MeV state (the 3.95 MeV peak is clearly asymmetric). The observed states at 1735 and 1772 keV in Ref. [16] were found to have large spectroscopic factors for $\nu d_{3/2}$ and $\nu s_{1/2}$ hole states but, due to limited experimental energy resolution, they were not able to resolve the two levels. In this work, with the excellent resolution of the high purity germanium detectors, we are able to assign accurate energies to the two. The shell-model calculations presented, found the $3/2^+$state at a higher energy than the $1/2^+$ state and as a result, we assign the 1735- and 1772-keV levels as $1/2^+$ and $3/2^+$, respectively. This is further confirmed by the branching ratio of the decays of the 3296-keV state as discussed ahead.

The 3296-keV state has the strongest population in the current β-decay study consistent with the previous study [29,43]. It has decay branches to the $7/2^-$ ground state, the 542-keV first excited $3/2^-$ state and a strong branch to the 1772-keV state which we propose to be the $3/2_1^+$ state. We could not identify any transition to the 1735-keV state within our observation capability. As the 3296-keV state decays to the ground state, it likely has a $5/2^+$ spin-parity. The vicinity of this state to the $5/2^+$ 3224-keV state predicted in the SM calculations ratifies this assignment and the calculated logft value of 4.98 justifies its strong population in the β decay. The predicted decay probabilities of the $5/2_1^+$ states to the $3/2_1^+$ and $1/2_1^+$ states in the SM calculations are listed in Table II. The decay

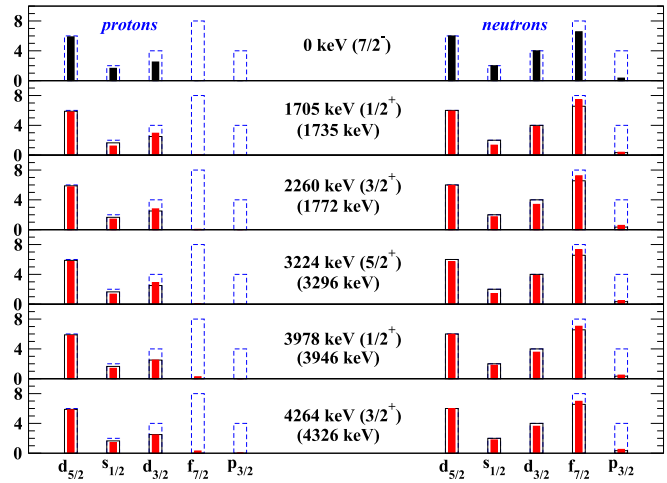

FIG. 9. The occupation number (y scale) of different orbitals (proton and neutron) for the positive parity excited states calculated from shell-model using the FSU interaction [30] for ^{45}Ar are shown. The energies of the experimental states corresponding to each proposed SM states in the present work are indicated in parentheses. The blue dashed columns are the maximum occupancy for an orbital $(2j+1)$. The solid black columns (and black solid lines) are the occupancy of the $7/2^-$ ground state and the red columns are the occupancies of the excited states of ^{45}Ar.

to the $3/2^+$ state via a $M1$ transition is stronger and supports the spin assignments to the doublet of states at ≈1.7 MeV.

The occupation numbers for the ground state and the excited positive-parity states in ^{45}Ar from SM calculations are shown in Fig. 9. The occupation numbers for the two states at ≈1.7 MeV clearly establish them as $\nu s_{1/2}$ and $\nu d_{3/2}$ hole states, respectively. The occupancy of the 3296-keV state from the shell-model calculation shows contribution from the $\nu d_{5/2}$ hole along with $s_{1/2}$. This level was also observed via the ^{1}H(^{46}Ar, ^{45}Ar) ^{2}H reaction by Lu *et al.* [16] though no spin was assigned to that state. The assignment of $5/2^+$ for 3296 keV from the present work, as discussed above, is consistent with the observation of a small peak at 3.29 MeV [16] in the deuteron spectra. Another state at 3.95 MeV, described to have $\ell = 0$ parentage in Ref. [16], is also observed in the present work. The shell-model calculation supports the presence of the second $1/2^+$ state at 3978 keV with considerable contribution from both neutron and proton $s_{1/2}$ orbitals. Therefore, the state at 3946 keV is assigned a $1/2^+$ spin-parity. The shell model further predicts a close by $3/2^+$ at 4264 keV (see Fig. 6), which we have associated with the 4326-keV state. The higher energy states (at 3978 keV and 4264 keV) show a rise in occupation number for protons in the $f_{7/2}$ orbital with respect to the ground-state configuration while the occupation number for $\pi d_{3/2}$ remains the same. It is accompanied by a slight drop in the occupancy for the $\nu f_{7/2}$ orbital. These states could have contribution from conversion of an $f_{7/2}$ neutron to a $f_{7/2}$ proton in the β decay.

2. Ground state of parent ^{45}Cl

The strong population of the $5/2^+$ at 3296 keV in the β decay leads to the determination of the ground state spin and

parity of the parent to be $3/2^+$. The ground-state spin-parity of the neutron-rich odd-mass Cl isotopes are in the spotlight due to the degeneracy of $\pi s_{1/2}$ and $\pi d_{3/2}$ orbitals as one moves from the $N = 20$ ^{37}Cl to the neutron-rich ^{45}Cl ($N = 28$). Gade *et al.* [12] systematically showed the reduction of the $E(1/2^+)$–$E(3/2^+)$ gap as a function of neutron-proton asymmetry for all the odd-mass K, Cl, and P isotopes. Though the ground-state spins have been experimentally verified for ^{41}Cl and ^{43}Cl as $1/2^+$ with a very close by $3/2^+$, the tentatively assigned $1/2^+$ ground state of ^{45}Cl based on SM calculations in Ref. [12] had not been confirmed experimentally. Two closely spaced energy states (127 keV apart) are predicted as candidates for the $1/2^+$ and $3/2^+$ generated from proton holes in $s_{1/2}$ and $d_{3/2}$, respectively. The present work reports the highest β feeding to the $5/2^+$ state in ^{45}Ar from the ground state (g.s.) of ^{45}Cl. This is possible only from a $3/2^+$ ground state and can be considered as the first experimental support for the assignment of $3/2^+$ spin to the ground state over $1/2^+$ for ^{45}Cl indicating a return of normal filling of orbitals in odd-A Cl isotopes. β decay of ^{45}S into ^{45}Cl can shed further light on the ground state spin/parity.

3. Negative parity states

The lower states in ^{45}Ar are supposed to have negative parity arising from the excitations of the odd neutron(s) within the fp shell. Their population in β decay is either due to feeding from the high-lying states or could also arise from first forbidden (FF) transitions.

The excited states at 1340 and 1418 keV are found to be consistent with the previous β-decay study by Mrazek *et al.* [29]. The state at 1.34 MeV was tentatively reported by Lu *et al.* [16] in a ^{1}H(^{46}Ar, d)^{45}Ar study though the ^{44}Ar(d, p)^{45}Ar reaction studied by Gaudefroy *et al.* [36,37] could not identify this state. Gaudefroy *et al.* on the other hand, reported a 1420(60)-keV excited state with $3/2^-$ spin-parity and described it as a member of the multiplet of the $\pi(2^+) \otimes \nu f_{7/2}$ configuration with one proton hole in $s_{1/2}$ and another in $d_{3/2}$. Because of the mixed nature, both these states were weakly populated in either of the transfer-reaction study [16,37]. The present shell-model calculation predicts the second excited state to be $3/2^-$ with a close by $1/2^-$ state (see Fig. 6). The 1340-keV level has a direct γ-decay branch to the $7/2^-$ ground state favoring a $3/2^-$ spin assignment over $1/2^-$ spin whereas the 1418-keV state decays to only the 542-keV $3/2^-$ state and not to the ground $7/2^-$ state. Therefore, it is proposed that the second excited state at 1340 keV has a $3/2^-$ spin-parity while the 1418-keV level is a $1/2^-$ consistent with the $\ell = 1$ assignment of Ref. [36] as well as present shell model predictions with a composite configuration of $\pi(d_{3/2} \otimes s_{1/2}) \otimes \nu p_{3/2}$.

The negative-parity energy levels in ^{45}Ar (observed here and from prior studies) and ^{43}Ar are further compared with the shell-model calculations in Fig. 10 to understand the evolution of the $N = 28$ shell gap. Relatively less information is available for the negative parity states in ^{43}Ar, as is clear in the figure. Unlike ^{45}Ar, a ground-state doublet of $5/2^-$ and $7/2^-$ is predicted in ^{43}Ar and can be considered as members of the multiplets arising from the configuration $\pi d_{3/2}^{-2} \nu f_{7/2}^{-3}$.

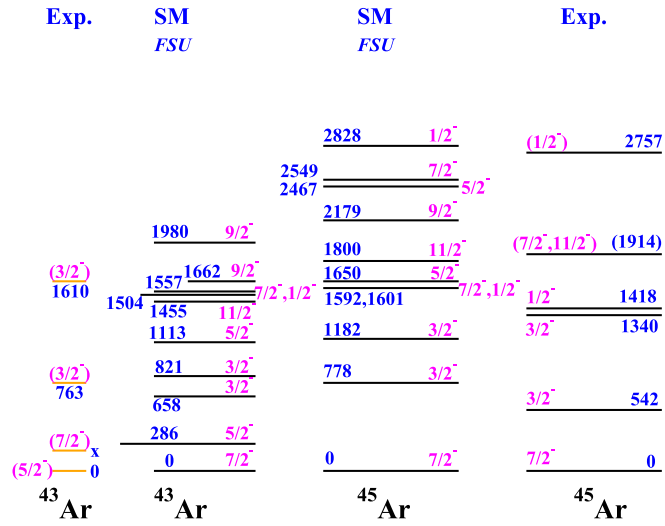

FIG. 10. The low-energy negative-parity states are displayed for ^{45}Ar and ^{43}Ar [38,42] for comparison both from experiment and shell-model calculations using the FSU interaction [30]. The experimental energy of $7/2^-$ state for ^{43}Ar is yet unknown.

There is only tentative experimental evidence of this doublet in ^{43}Ar with $5/2^-$ proposed to be the ground state [38,39]. Further the β decay of ^{43}Cl with a $3/2^+$ g.s. [40] shows a large branch to the ground state of ^{43}Ar through FF decay which also favors the $5/2^-$ assignment. Hence, though the SM calculations using the FSU interaction correctly predict very closely spaced $7/2^-$(g.s.) and $5/2^-$ state (286 keV in Fig. 10) for ^{43}Ar, the $5/2^-$ is more probable for the ground state. For ^{45}Ar on the other hand, both the SM calculations and the experimental observations do not support a close $5/2^-$–$7/2^-$ ground-state multiplet, a signature of the proximity to the $N = 28$ shell closure.

B. ^{44}Ar

The states populated in ^{44}Ar follow the neutron emission from the $1p1h$ positive parity states with spins of 1/2, 3/2, or 5/2 populated in ^{45}Ar above S_n. The first excited state of even-even ^{44}Ar is at 1158 keV with a J^π of 2^+ known from earlier Coulomb-excitation, in-beam γ-spectroscopy and deep inelastic studies [17,18,31,32] and is described as a deformed state while the second excited one is also a 2^+ state at 2011 keV. The spins of the other excited levels observed at 2978, 4808, and 5354 keV are proposed to be 0^+ to 4^+ in National Nuclear Data Center (NNDC) [41]. We have tried to make more specific spin assignments to these states assuming their positive parity by comparing with the predictions of shell-model calculations in the $0p0h$ valence space. As depicted in Fig. 1 the neutron will be emitted from the sd shell (if the final state is positive parity) leading to a $2p2h$ state. Thus the positive parity states populated in ^{44}Ar following β-delayed neutron emission will have some admixture of $2p2h$ configuration to facilitate the transition. Our calculations currently cannot accommodate mixed calculations.

The experimental levels (left panel) and SM predicted states (right panel) for ^{44}Ar are shown in Fig. 8 along with the

relative intensities of the γ transitions from each level. The experimental 2978-keV level decays to the first and second 2^+ states via the 1818- and 966-keV transitions, respectively, where the 966-keV decay dominates over the 1818-keV branch. This 2978-keV level lies close in energy to four predicted states (0^+, 4^+, 2^+, and 3^+). The calculated 4^+ (2978 keV) and 2^+ (3013 keV) states have higher transition rates to the 4_1^+ (2680 keV) and 0^+ (g.s.) states, respectively, which is not observed in the decay of the experimental 2978-keV level. This leaves the two spins, 3^+ (3047 keV) and 0^+ (2717 keV), as the most probable candidates for this level.

The level at 4808 keV decays to the ground state and the excited 2^+ (1158- and 2011-keV) states. Therefore, among the prior suggested spin-parity assignments, 4^+, 3^+, or 0^+ [41] are not possible for this state. Between the remaining 2^+ and 1^+ spin, the shell model does not predict any 1^+ state nearby (Fig. 8), therefore the spin for this level is suggested to be 2^+ corresponding to the level 4842 keV from the calculation. Further, the calculations (Fig. 8) predict that the 4842-keV level (experimental 4808 keV level) has the most intense decay branch to the ground state and the excited 2^+ states, which matches with the experimental observation. If the spin-parity of 2978-keV state is assigned as 3^+ then the shell-model predicts a strongest decay branch from 4808-keV to 2978-keV level. The absence of a decay path from 4808-keV to 2978-keV state encourages us to assign the 2978-keV state as the excited 0^+ over the 3^+ possibility. The systematics of excited 0^+ in Ar isotopes will be discussed next.

The highest observed level from the present βn decay work is at 5354 keV with a decay only to the newly assigned 0^+ 2978-keV level. This 5354-keV level was proposed to decay to the 2011-keV (2_2^+) and 1158-keV (2_1^+) states via the 3342- and 4195-keV transitions in the earlier ^{44}Cl β-decay work [29] but with 3–5 times less intensity than the 2376 keV transition. The observation of the strong 2376-keV transition to the 2978-keV (0^+) state rules out 0^+ and 3^+ assignments for the 5354 keV level. The shell model predicts a 2^+ at 5141 keV and a 1^+ at 5208, both of which are good candidates but the 2^+ is predicted to decay by a strong transition to the 2_2^+ state not consistent with the experiment. Therefore, the 5354 keV is assigned as 1^+, consistent with all experimental observations. The population of 1^+ and 2^+ in the delayed neutron decay suggests the population of a $3/2^+$ unbound state in ^{45}Ar which decays by a $\ell = 0$ neutron.

C. Even-even isotopes near $N = 28$

To understand the evolution of shape away from the $N = 28$ shell closure, the excited state energies of 2_1^+ and 0_2^+ excited states are plotted for even-even Ar isotopes as a function of neutron number in Fig. 11. With $N = 20$, both 2_1^+ and 0_2^+ are high in energy for ^{38}Ar, reflecting the large shell gap between the $d_{3/2}$ and $f_{7/2}$ orbitals. As we increase the neutron number approaching the half-occupancy of the $f_{7/2}$ orbital, the lowering of the first 2^+ state indicates an increasing collectivity, and reduction of the $N = 28$ shell gap. In the Ar isotopic chain, it is interesting to notice that the most collective behavior is for the ground state of ^{44}Ar ($N = 26$) signified by the lowest energy of 2_1^+. After that, the increase of the

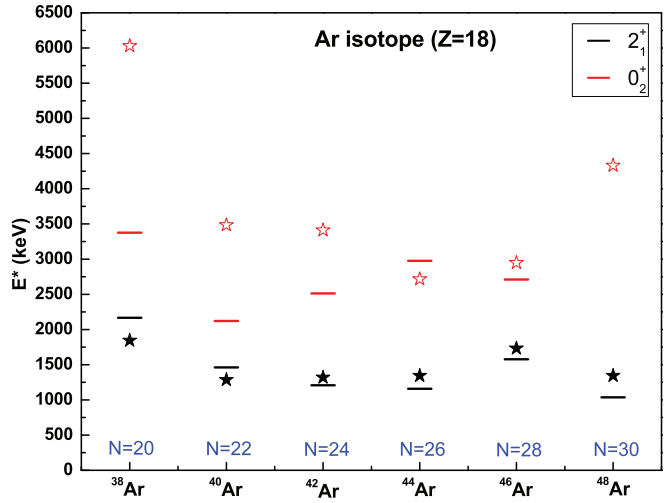

FIG. 11. The experimental low-lying 2_1^+ and 0_2^+ energies of Ar isotopes as a function of neutron number. The shell-model (using the FSU interaction) predicted states are also shown as closed (open) stars for 2_1^+ (0_2^+) spin. The 0_2^+ spin for ^{42}Ar is adopted from one of the possible spins predicted in NNDC [42] for the 2512.5-keV level for comparison purposes. The experimental values for the nuclei (other than ^{44}Ar) are taken from Refs. [18,38,42,44–46].

2_1^+ energy points towards the restoration of the shell gap between the $\nu f_{7/2}$ and $\nu p_{3/2}$ orbitals in ^{46}Ar. With an additional neutron pair above $N = 28$, the 2^+ state comes down in energy for ^{48}Ar.

A different trend is seen for the 0_2^+ state, which generally represents a different shape of the nucleus from the ground state. For ^{40}Ar, the 0_2^+ state is described to be part of a superdeformed band in Ref. [47]. With increasing neutron number, the energy of this state is found to increase, attaining a maximum value for ^{44}Ar. After that, the experimental 0_2^+ state shows a decreasing trend again for ^{46}Ar. As can be seen from Fig. 11, the shell-model calculations with the FSU interaction (solid black stars) closely mirror the 2_1^+ values for $^{38-48}$Ar. For the 0_2^+ states (open red star) from $0p0h$ configurations, the shell-model predictions show an increasing trend in energy with decreasing neutron number, in disagreement with the experiment. A possible reason is that the 0_2^+ states for $^{38-42}$Ar isotopes could have contribution from $2p2h$ configuration which is beyond the scope of present SM calculations. It will be interesting to search for the 0_2^+ state in ^{48}Ar, which is predicted to be very high (4.3 MeV) in the present SM calculation.

V. SUMMARY

The β^- decay of ^{45}Cl is reported here, from an experiment performed at the NSCL following the fragmentation of a ^{48}Ca primary beam. The half-life of ^{45}Cl is measured to be 513(36) ms, which is longer than the prior measurement from GANIL but consistent with shell model calculations using the FSU interaction. The level schemes of ^{45}Ar and ^{44}Ar are established from the observed γ-γ coincidences in the β and $\beta 1n$ channels, respectively. Many of the prior

tentative placements of transitions in ^{45}Ar have been verified and a new γ transition at 2554 keV has been added. The experimentally observed levels are compared with SM calculations for both ^{44,45}Ar with excellent agreement. From the predicted occupancy of different orbitals and the decay pattern of the γ transitions from the excited levels, the spin-parity of the levels of ^{45}Ar populated via GT transitions are proposed. The higher lying positive-parity states of ^{45}Ar are candidates for $1p1h$ excitations consistent with their population in prior transfer reactions. The maximum feeding to the $5/2^+$ state in ^{45}Ar, supported by the small $\log ft$ value calculated from SM calculations, allowed us to assign a spin-parity of $3/2^+$ to the ground state of the parent ^{45}Cl. The spin and parity for the levels in ^{44}Ar are proposed by comparing with SM calculations. An excited 0_2^+ state is proposed for the first time in ^{44}Ar at 2978 keV. The SM calculations reproduce the experimental evolution of the 2_1^+ state for the even-A Ar isotopes (from $N = 20$ to 30) reasonably well and suggest maximum collectivity for the ground state of ^{44}Ar. However, the trend of the excited 0_2^+ in even-even Ar isotopes is not that consistent with the calculations. The accuracy of the present shell model calculations for predicting the 0_2^+ states will get validation with the experimental observation of the yet unknown 0_2^+ state for ^{48}Ar in future experimental endeavors.

ACKNOWLEDGMENTS

We thank the NSCL operation team and the A1900 team, especially Tom Ginter, for the production and optimization of the secondary beam. This work was supported by the U.S. National Science Foundation under Grant No. PHY-2012522 (FSU), No. PHY-1848177 (CAREER); U.S. Department of Energy, Office of Science, Office of Nuclear Physics under Award No. DE-SC0020451 (FRIB), No. DE-FG02-94ER40848 (UML), No. DE-AC52-07NA27344 (LLNL), No. DE-AC02-06CH11357(ANL), and also by the U.S. Department of Energy (DOE) National Nuclear Security Administration Grant No. DOE-DE-NA0003906, and the Nuclear Science and Security Consortium under Award No. DE-NA0003180.

[1] D. Warner, Not-so-magic numbers, Nature (London) **430**, 517 (2004).
[2] B. Brown, The nuclear shell model towards the drip lines, Prog. Part. Nucl. Phys. **47**, 517 (2001).
[3] O. Sorlin and M.-G. Porquet, Nuclear magic numbers: New features far from stability, Prog. Part. Nucl. Phys. **61**, 602 (2008).
[4] S. Calinescu, L. Cáceres, S. Grévy, O. Sorlin, Z. Dombrádi, M. Stanoiu, R. Astabatyan, C. Borcea, R. Borcea, M. Bowry, W. Catford, E. Clément, S. Franchoo, R. Garcia, R. Gillibert, I. H. Guerin, I. Kuti, S. Lukyanov, A. Lepailleur, V. Maslov *et al.*, Coulomb excitation of ^{44}Ca and ^{46}Ar, Phys. Rev. C **93**, 044333 (2016).
[5] B. Bastin, S. Grévy, D. Sohler, O. Sorlin, Z. Dombrádi, N. L. Achouri, J. C. Angélique, F. Azaiez, D. Baiborodin, R. Borcea, C. Bourgeois, A. Buta, A. Bürger, R. Chapman, J. C. Dalouzy, Z. Dlouhy, A. Drouard, Z. Elekes, S. Franchoo, S. Iacob *et al.*, Collapse of the $N = 28$ Shell Closure in ^{42}Si, Phys. Rev. Lett. **99**, 022503 (2007).
[6] C. Force, S. Grévy, L. Gaudefroy, O. Sorlin, L. Cáceres, F. Rotaru, J. Mrazek, N. L. Achouri, J. C. Angélique, F. Azaiez, B. Bastin, R. Borcea, A. Buta, J. M. Daugas, Z. Dlouhy, Z. Dombrádi, F. De Oliveira, F. Negoita, Y. Penionzhkevich, M. G. Saint-Laurent *et al.*, Prolate-Spherical Shape Coexistence at $N = 28$ in ^{44}S, Phys. Rev. Lett. **105**, 102501 (2010).
[7] J. J. Parker, I. Wiedenhöver, P. D. Cottle, J. Baker, D. McPherson, M. A. Riley, D. Santiago-Gonzalez, A. Volya, V. M. Bader, T. Baugher, D. Bazin, A. Gade, T. Ginter, H. Iwasaki, C. Loelius, C. Morse, F. Recchia, D. Smalley, S. R. Stroberg, K. Whitmore *et al.*, Isomeric Character of the Lowest Observed 4^+ State in ^{44}S, Phys. Rev. Lett. **118**, 052501 (2017).
[8] T. Otsuka, A. Gade, O. Sorlin, T. Suzuki, and Y. Utsuno, Evolution of shell structure in exotic nuclei, Rev. Mod. Phys. **92**, 015002 (2020).
[9] T. Glasmacher, B. Brown, M. Chromik, P. Cottle, M. Fauerbach, R. Ibbotson, K. Kemper, D. Morrissey, H. Scheit, D. Sklenicka, and M. Steiner, Collectivity in ^{44}S, Phys. Lett. B **395**, 163 (1997).
[10] T. R. Werner, J. A. Sheikh, W. Nazarewicz, M. R. Strayer, A. S. Umar, and M. Misu, Shape coexistence around $_{16}{}^{44}S_{28}$: The deformed $N = 28$ region 1565, Phys. Lett. B **335**, 259 (1994).
[11] B. Longfellow, D. Weisshaar, A. Gade, B. A. Brown, D. Bazin, K. W. Brown, B. Elman, J. Pereira, D. Rhodes, and M. Spieker, Quadrupole collectivity in the neutron-rich sulfur isotopes ^{38,40,42,44}S, Phys. Rev. C **103**, 054309 (2021).
[12] A. Gade, B. A. Brown, D. Bazin, C. M. Campbell, J. A. Church, D. C. Dinca, J. Enders, T. Glasmacher, M. Horoi, Z. Hu, K. W. Kemper, W. F. Mueller, T. Otsuka, L. A. Riley, B. T. Roeder, T. Suzuki, J. R. Terry, K. L. Yurkewicz, and H. Zwahlen, Evolution of the $E(1/2_1^+) - E(3/2_1^+)$ energy spacing in odd-mass K, Cl, and P isotopes for $N = 20 - 28$, Phys. Rev. C **74**, 034322 (2006).
[13] T. Otsuka, T. Suzuki, R. Fujimoto, H. Grawe, and Y. Akaishi, Evolution of Nuclear Shells due to the Tensor Force, Phys. Rev. Lett. **95**, 232502 (2005).
[14] S. R. Stroberg, A. Gade, T. Baugher, D. Bazin, B. A. Brown, J. M. Cook, T. Glasmacher, G. F. Grinyer, S. McDaniel, A. Ratkiewicz, and D. Weisshaar, In-beam γ-ray spectroscopy of $^{43-46}$Cl, Phys. Rev. C **86**, 024321 (2012).
[15] K. Blaum, W. Geithner, J. Lassen, P. Lievens, K. Marinova, and R. Neugart, Nuclear moments and charge radii of argon isotopes between the neutron-shell closures $N = 20$ and $N = 28$, Nucl. Phys. A **799**, 30 (2008).
[16] F. Lu, J. Lee, M. B. Tsang, D. Bazin, D. Coupland, V. Henzl, D. Henzlova, M. Kilburn, W. G. Lynch, A. M. Rogers, A. Sanetullaev, Z. Y. Sun, M. Youngs, R. J. Charity, L. G. Sobotka, M. Famiano, S. Hudan, M. Horoi, and Y. L. Ye, Neutron-hole states in ^{45}Ar from ^{1}H(^{46}Ar, d) ^{45}Ar reactions, Phys. Rev. C **88**, 017604 (2013).
[17] M. Zielińska, A. Görgen, E. Clément, J. P. Delaroche, M. Girod, W. Korten, A. Bürger, W. Catford, C. Dossat, J. Iwanicki, J. Libert, J. Ljungvall, P. J. Napiorkowski, A. Obertelli, D. Pietak,

R. Rodríguez-Guzmán, G. Sletten, J. Srebrny, C. Theisen, and K. Wrzosek, Shape of ^{44}Ar: Onset of deformation in neutron-rich nuclei near ^{48}Ca, Phys. Rev. C **80**, 014317 (2009).

[18] H. Scheit, T. Glasmacher, B. A. Brown, J. A. Brown, P. D. Cottle, P. G. Hansen, R. Harkewicz, M. Hellström, R. W. Ibbotson, J. K. Jewell, K. W. Kemper, D. J. Morrissey, M. Steiner, P. Thirolf, and M. Thoennessen, New Region of Deformation: The Neutron-Rich Sulfur Isotopes, Phys. Rev. Lett. **77**, 3967 (1996).

[19] A. Gade, D. Bazin, C. M. Campbell, J. A. Church, D. C. Dinca, J. Enders, T. Glasmacher, Z. Hu, K. W. Kemper, W. F. Mueller, H. Olliver, B. C. Perry, L. A. Riley, B. T. Roeder, B. M. Sherrill, and J. R. Terry, Detailed experimental study on intermediate-energy coulomb excitation of ^{46}Ar, Phys. Rev. C **68**, 014302 (2003).

[20] D. Mengoni, J. J. Valiente-Dobón, A. Gadea, S. Lunardi, S. M. Lenzi, R. Broda, A. Dewald, T. Pissulla, L. J. Angus, S. Aydin, D. Bazzacco, G. Benzoni, P. G. Bizzeti, A. M. Bizzeti-Sona, P. Boutachkov, L. Corradi, F. Crespi, G. de Angelis, E. Farnea, E. Fioretto *et al.*, Lifetime measurements of excited states in neutron-rich ^{44,46}Ar populated via a multinucleon transfer reaction, Phys. Rev. C **82**, 024308 (2010).

[21] A. Gade and B. Sherill, NSCL and FRIB at Michigan State University: Nuclear science at the limits of stability, Phys. Scr. **91**, 053003 (2016).

[22] D. Morrissey, B. Sherrill, M. Steiner, A. Stolz, and I. Wiedenhoever, Commissioning the A1900 projectile fragment separator, Nucl. Instrum. Methods Phys. Res. B **204**, 90 (2003), 14th International Conference on Electromagnetic Isotope Separators and Techniques Related to their Applications.

[23] J. Prisciandaro, A. Morton, and P. Mantica, Beta counting system for fast fragmentation beams, Nucl. Instrum. Methods Phys. Res. A **505**, 140 (2003), Proceedings of the Tenth Symposium on Radiation Measurements and Applications.

[24] B. M. Coursey, D. D. Hoppes, and F. J. Schima, NSCL SRM source, Nucl. Instrum. Methods Phys. Res. **193**, 1 (1982).

[25] C. Prokop, S. Liddick, B. Abromeit, A. Chemey, N. Larson, S. Suchyta, and J. Tompkins, Digital data acquisition system implementation at the National Superconducting Cyclotron Laboratory, Nucl. Instrum. Methods Phys. Res. A **741**, 163 (2014).

[26] V. Tripathi, S. Bhattacharya, E. Rubino, C. Benetti, J. F. Perello, S. L. Tabor, S. N. Liddick, P. C. Bender, M. P. Carpenter, J. J. Carroll, A. Chester, C. J. Chiara, K. Childers, B. R. Clark, B. P. Crider, J. T. Harke, B. Longfellow, R. S. Lubna, S. Luitel, T. H. Ogunbeku *et al.*, β^- decay of exotic P and S isotopes with neutron number near 28, Phys. Rev. C **106**, 064314 (2022).

[27] O. Sorlin, D. Guillemaud-Mueller, A. C. Mueller, V. Borrel, S. Dogny, F. Pougheon, K.-L. Kratz, H. Gabelmann, B. Pfeiffer, A. Wöhr, W. Ziegert, Y. E. Penionzhkevich, S. M. Lukyanov, V. S. Salamatin, R. Anne, C. Borcea, L. K. Fifield, M. Lewitowicz, M. G. Saint-Laurent, D. Bazin *et al.*, Decay properties of exotic $N \simeq 28$ S and Cl nuclei and the ^{48}Ca / ^{46}Ca abundance ratio, Phys. Rev. C **47**, 2941 (1993).

[28] J. A. Winger, H. H. Yousif, W. C. Ma, V. Ravikumar, Y. W. Lui, S. K. Phillips, R. B. Piercey, P. F. Mantica, B. Pritychenko, R. M. Ronningen, and M. Steiner, Low-energy structure of neutron-rich S, Cl and Ar nuclides through β decay, in *Proceedings of the Exotic Nuclei and Atomic Masses (ENAM 98) 23–27 Jun 1998, Bellaire, Michigan*, AIP Conf. Proc. 455 (AIP, Melville, NY, 1998), pp. 606–609.

[29] J. Mrázek, S. Grévy, S. Iulian, A. Buta, F. Negoita, J. Angélique, P. Baumann, C. Borcea, G. Canchel, W. Catford, S. Courtin, J. Daugas, Z. Dlouhý, P. Dessagne, A. Knipper, G. Lehrsenneau, F. Lecolley, J. Lecouey, M. Lewitowicz, E. Liénard *et al.*, Study of neutron-rich argon isotopes in β-decay, Nucl. Phys. A **734**, E65 (2004), Proceedings of the Eighth International Conference on Nucleus-Nucleus Collisions (NN2003).

[30] R. S. Lubna, K. Kravvaris, S. L. Tabor, V. Tripathi, E. Rubino, and A. Volya, Evolution of the $N = 20$ and 28 shell gaps and two-particle-two-hole states in the FSU interaction, Phys. Rev. Res. **2**, 043342 (2020).

[31] S. Wan, J. Gerl, J. Cub, J. Holeczek, P. Reiter, D. Schwalm, T. Aumann, K. Boretzky, W. Dostal, B. Eberlein, H. Emling, C. Ender, T. Elze, H. Geissel, A. Grunschlob, R. Holzmann, N. Iwasa, M. Kaspar, A. Kleinbohl, O. Koschorrek *et al.*, In-beam γ-spectroscopy with relativistic radioactive ion beams, Eur. Phys. J. A **6**, 167 (1999).

[32] B. Fornal, R. Broda, W. Królas, T. Pawlat, J. Wrzesi'nski, D. Bazzacco, S. Lunardi, C. Rossi Alvarez, G. Viesti, G. de Angelis, M. Cinausero, D. Napoli, J. Gerl, E. Caurier, and F. Nowacki, New states in ^{44,46}Ar isotopes from deep-inelastic heavy ion reaction studies, Eur. Phys. J. A **7**, 147 (2000).

[33] A. Volya, Continuum shell model code, https://www.volya.net/ (2016).

[34] A. Gade, B. A. Brown, D. Weisshaar, D. Bazin, K. W. Brown, R. J. Charity, P. Farris, A. M. Hill, J. Li, B. Longfellow, D. Rhodes, W. Reviol, and J. A. Tostevin, Dissipative Reactions with Intermediate-Energy Beams: A Novel Approach to Populate Complex-Structure States in Rare Isotopes, Phys. Rev. Lett. **129**, 242501 (2022).

[35] B. A. Brown, The nuclear shell model towards the drip lines, Physics **4**, 525 (2022).

[36] L. Gaudefroy, O. Sorlin, D. Beaumel, Y. Blumenfeld, Z. DombrÃ¡di, S. Fortier, S. Franchoo, M. Gélin, J. Gibelin, S. Grévy, F. Hammache, F. Ibrahim, K. Kemper, K. L. Kratz, S. M. Lukyanov, C. Monrozeau, L. Nalpas, F. Nowacki, A. N. Ostrowski, Y.-E. Penionzhkevich *et al.*, Study of ^{45}Ar through (d, p) reaction at spiral, J. Phys. G: Nucl. Part. Phys. **31**, S1623 (2005).

[37] L. Gaudefroy, O. Sorlin, F. Nowacki, D. Beaumel, Y. Blumenfeld, Z. Dombrádi, S. Fortier, S. Franchoo, S. Grévy, F. Hammache, K. W. Kemper, K. L. Kratz, M. G. St. Laurent, S. M. Lukyanov, L. Nalpas, A. N. Ostrowski, Y.-E. Penionzhkevich, E. C. Pollacco, P. Roussel, P. Roussel-Chomaz *et al.*, Structure of the $N = 27$ isotones derived from the ^{44}Ar$(d, p)^{45}$Ar reaction, Phys. Rev. C **78**, 034307 (2008).

[38] S. Szilner, L. Corradi, F. Haas, D. Lebhertz, G. Pollarolo, C. A. Ur, L. Angus, S. Beghini, M. Bouhelal, R. Chapman, E. Caurier, S. Courtin, E. Farnea, E. Fioretto, A. Gadea, A. Goasduff, D. Jelavić-Malenica, V. Kumar, S. Lunardi, N. Mărginean *et al.*, Interplay between single-particle and collective excitations in argon isotopes populated by transfer reactions, Phys. Rev. C **84**, 014325 (2011).

[39] F. Maréchal, T. Suomijärvi, Y. Blumenfeld, A. Azhari, D. Bazin, J. A. Brown, P. D. Cottle, M. Fauerbach, T. Glasmacher, S. E. Hirzebruch, J. K. Jewell, J. H. Kelley, K. W. Kemper, P. F. Mantica, D. J. Morrissey, L. A. Riley, J. A. Scarpaci, H. Scheit, and M. Steiner, Proton scattering from the unstable neutron-rich nucleus ^{43}Ar, Phys. Rev. C **60**, 064623 (1999).

[40] J. A. Winger, P. F. Mantica, and R. M. Ronningen, β decay of ^{40,42}S and ^{43}Cl, Phys. Rev. C **73**, 044318 (2006).

[41] C. Jun, B. Singh, and J. A. Cameron, (2001) https://www.nndc.bnl.gov/nudat3/.
[42] NNDC, https://www.nndc.bnl.gov/nudat3/ (2005).
[43] T. W. Burrows, ENSDF data, NDS **171**, 109 (2008).
[44] K.-H. Speidel, S. Schielke, J. Leske, J. Gerber, P. Maier-Komor, S. Robinson, Y. Sharon, and L. Zamick, Experimental g factors and B(E2) values in Ar isotopes: Crossing the $N=20$ semi-magic divide, Phys. Lett. B **632**, 207 (2006).
[45] K.-H. Speidel, S. Schielke, J. Leske, N. Pietralla, T. Ahn, A. Costin, O. Zell, J. Gerber, P. Maier-Komor, S. J. Q. Robinson, A. Escuderos, Y. Y. Sharon, and L. Zamick, New shell model calculations for ^{40}Ar based on recent *g*-factor and lifetime measurements, Phys. Rev. C **78**, 017304 (2008).
[46] S. Bhattacharyya, M. Rejmund, A. Navin, E. Caurier, F. Nowacki, A. Poves, R. Chapman, D. O'Donnell, M. Gelin, A. Hodsdon, X. Liang, W. Mittig, G. Mukherjee, F. Rejmund, M. Rousseau, P. Roussel-Chomaz, K.-M. Spohr, and C. Theisen, Structure of Neutron-Rich Ar Isotopes Beyond $N=28$, Phys. Rev. Lett. **101**, 032501 (2008).
[47] E. Ideguchi, S. Ota, T. Morikawa, M. Oshima, M. Koizumi, Y. Toh, A. Kimura, H. Harada, K. Furutaka, S. Nakamura, F. Kitatani, Y. Hatsukawa, T. Shizuma, M. Sugawara, H. Miyatake, Y. Watanabe, Y. Hirayama, and M. Oi, Superdeformation in asymmetric $N > Z$ nucleus ^{40}Ar, Phys. Lett. B **686**, 18 (2010).